

https://doi.org/10.1070/QEL16424

ABC-model analysis of gain-switched pulse characteristics in low-dimensional semiconductor lasers

Xumin Bao, Yuejun Liu, Guoen Weng, Xiaobo Hu, Shaoqiang Chen

Abstract. **The gain-switching dynamics of low-dimensional semiconductor lasers is simulated numerically by using a two-dimensional rate-equation model. Use is also made of the *ABC* model, where the carrier recombination rate is described by a function of carrier densities including Shockley–Read–Hall (SRH) recombination coefficient *A*, spontaneous emission coefficient *B* and Auger recombination coefficient *C*. Effects of the *ABC* parameters on the ultrafast gain-switched pulse characteristics with high-density pulse excitation are analysed. It is found that while the parameter *A* has almost no obvious effects, the parameters *B* and *C* have distinctly different effects: *B* influences significantly the delay time of the gain-switched pulse, while *C* affects mainly the pulse intensity.**

Keywords: *rate equation, gain-switching, Auger recombination, semiconductor laser.*

1. Introduction

Compact, stable, low-cost and short-pulse semiconductor lasers have a wide range of applications such as laser systems, optical measurements, LiFi systems [1, 2], integrated optics and optical storages [3–5]. Quantum-well or quantum-dot based low-dimensional semiconductor lasers have the advantages of low threshold and controllable lasing wavelength [6–9], and short pulses generated by semiconductor lasers under gain-switching operation have the advantages of low-cost and tunable operation frequency [10–12]. Although the gain-switching technique has been widely studied [13–16], it is still not well used in real applications due to the low power and long pulse duration (several tens of picoseconds) [11, 17]. In order to promote their applications, gain-switched semiconductor lasers should generate short pulses with high power and short duration, which is generally achieved under high-density pulsed current injection [14, 18, 19] or pulsed optical pumping [15, 16, 20].

Carrier recombination processes play an important role in the optical properties of optoelectronic materials and devices. It is reported [21, 22] that the external quantum efficiency drop mechanism in GaInN/GaN LEDs with high current injection is likely caused by Auger recombination processes rather than by the dislocation density. It is also reported [23] that Auger recombination can strongly increase the threshold current and limit the power conversion efficiency of high-power GaN-based lasers. In order to understand and consequently improve the performance of high power semiconductor lasers, it is of great importance to study the effects of carrier recombination processes on the lasing performance of semiconductor lasers with high output powers.

We have previously constructed a two-dimensional semiconductor laser rate equation model including gain saturation effects to simulate and analyse the gain-switching properties of semiconductor lasers [20, 24]. The practicability of the model has been well demonstrated with successful design and product of 2-ps short pulses via gain-switched semiconductor lasers [16, 20]. In that model, the carrier lifetime was assumed to be constant during gain-switching, and the separate effects of the *ABC* parameters [Shockley–Read–Hall (SRH) recombination coefficient *A*, spontaneous emission coefficient *B* and Auger recombination coefficient *C*] as functions of carrier density were not taken into account.

In this paper, in order to investigate the effects of the *ABC* parameters on the pulse generation dynamics in gain-switched low-dimensional semiconductor lasers with high density excitation, we modified the single-mode rate equation with the *ABC* model, and then analysed gain-switching characteristics of semiconductor lasers with different *ABC* parameters. We demonstrated that the delay time, pulse intensity and full width at half maximum of gain-switched output pulses can be affected significantly by the spontaneous emission coefficient *B* and Auger recombination coefficient *C*. Temporal evolutions of the photon density and carrier density with different values of the *ABC* parameters were also presented for in-depth understanding of the influence of the parameters.

2. Simulation model

We use the following rate equation including *ABC* parameters for simulation [24, 25]:

$$\frac{\mathrm{d}n^{2\mathrm{D}}}{\mathrm{d}t} = n^{2\mathrm{D}}_{\mathrm{pump}}\xi(t) - \frac{\Gamma}{m}v_{\mathrm{g}}g\frac{s^{2\mathrm{D}}}{1+\varepsilon s^{2\mathrm{D}}} - A_{2\mathrm{D}}n^{2\mathrm{D}} - B_{2\mathrm{D}}(n^{2\mathrm{D}})^2 - C_{2\mathrm{D}}(n^{2\mathrm{D}})^3, \quad (1)$$

$$\frac{\mathrm{d}s^{2\mathrm{D}}}{\mathrm{d}t} = \Gamma v_{\mathrm{g}}g\frac{s^{2\mathrm{D}}}{1+\varepsilon s^{2\mathrm{D}}} - \frac{s^{2\mathrm{D}}}{\tau_{\mathrm{p}}} + m\beta B_{2\mathrm{D}}(n^{2\mathrm{D}})^2, \quad (2)$$

$$g(g_{\mathrm{s}}, g_0, n_0^{2\mathrm{D}}) = g_0(n^{2\mathrm{D}} - n_0^{2\mathrm{D}})\left[1 + \frac{g_0(n^{2\mathrm{D}} - n_0^{2\mathrm{D}})}{g_{\mathrm{s}}}\right]^{-1}, \quad (3)$$

Xumin Bao, Yuejun Liu, Guoen Weng, Xiaobo Hu, Shaoqiang Chen
Department of Electronic Engineering, East China Normal University, 500 Dongchuan Road, Shanghai 200241, China;
e-mail: sqchen@ee.ecnu.edu.cn

Received 5 March 2017; revision received 12 July 2017
Kvantovaya Elektronika **48** (1) 7–12 (2018)
Submitted in English

where s^{2D} is the two-dimensional (2D) photon density for all active layers; n^{2D} is the 2D carrier density per single active layer; n^{2D}_{pump} is the time-integrated injected carrier density per single active layer; $\xi(t)$ is the normalised time trace of the pump pulse; m is the active layer number; Γ is the confinement factor; v_g is the group velocity; $g(g_s, g_0, n_0^{2D})$ is the nonlinear material gain model defined by a function of g_s (saturated gain), g_0 (differential gain) and n_0^{2D} (transparency density); τ_p is the photon lifetime; ε is the gain compression factor; and β is the spontaneous coupling factor.

In the numerical simulations, we used the following parameters: $n_0^{2D} = 0.7\times10^{12}$ cm^{-2}; $n^{2D}_{pump} = 2.94\times10^{12}$ cm^{-2}, which is 10 times greater than the threshold value; $\tau_p = 3.7$ ps; $v_g = 8.57\times10^{-3}$ cm ps^{-1}; and $\beta = 5.0\times10^{-5}$. A Gaussian function with a pulse duration of 2 ps is assumed for $\xi(t)$ as a pump light source. We varied the variables respectively in the

Table 1. Values and the variation range of simulation variables.

Parameter	Variation range
$\varepsilon = 0$	$(0-0.15)\times10^{-12}$ cm^2
$g_s = 1100$ cm^{-1}	1030–16950 cm^{-1}
$g_0 = 3\times10^{-9}$ cm	$(1-15)\times10^{-9}$ cm
$A = 4.5\times10^{6}$ s^{-1}	10^6-10^7 s^{-1}
$B = 2.31\times10^{-5}$ cm^2 s^{-1}	$10^{-7}-10^{-5}$ cm^2 s^{-1}
$C = 7.3\times10^{-18}$ cm^4 s^{-1}	$10^{-23}-10^{-17}$ cm^4 s^{-1}

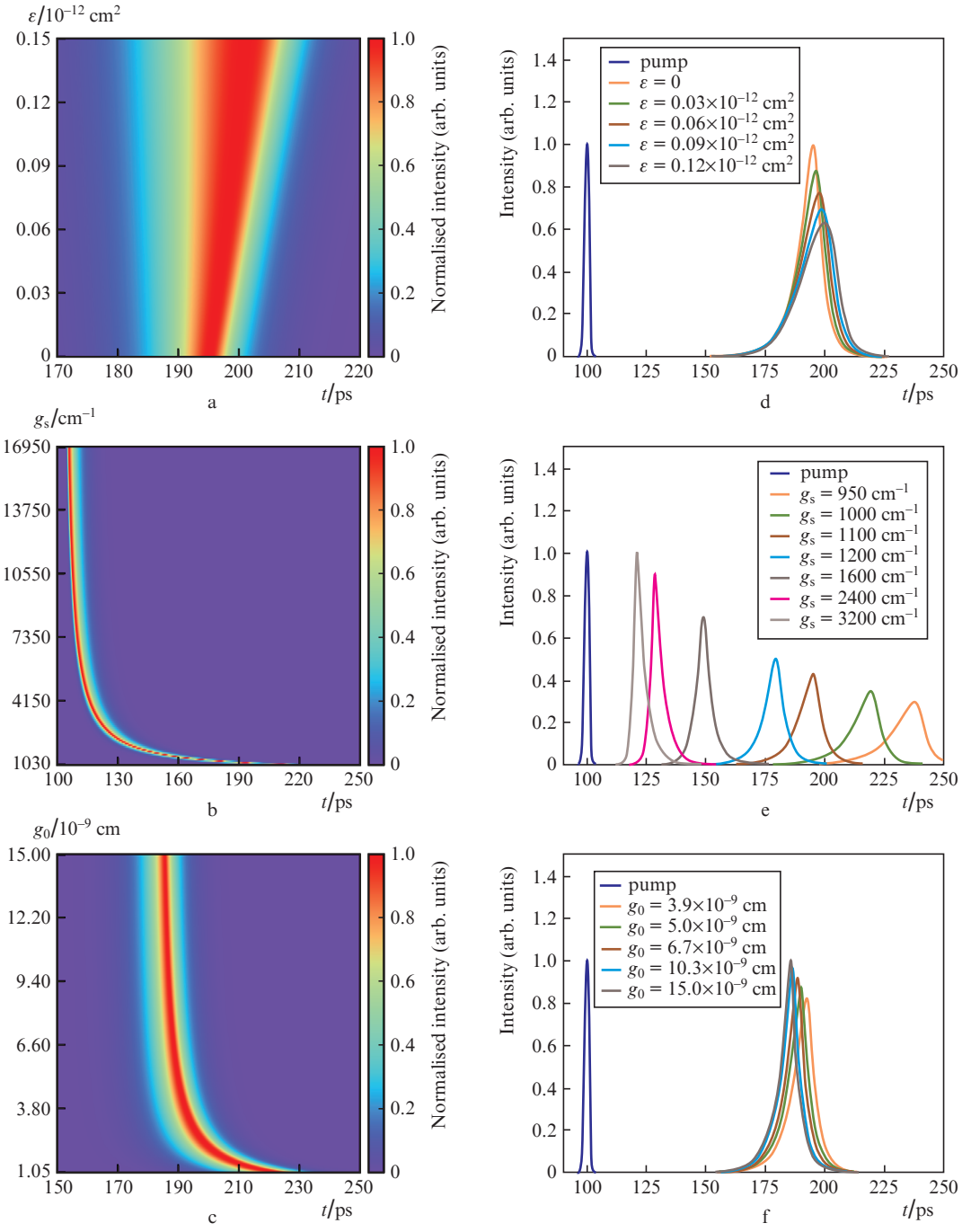

Figure 1. (Colour online) (a–c) Temporal evolution of normalised photon density and (d–f) output waveforms at different values of ε, g_s and g_0.

fixed range shown in Table 1 to investigate their effects on gain-switched pulse characteristics [21, 24, 26–29].

3. Results and discussion

The effects of ε, g_s, g_0, A, B and C on gain-switched pulse generation are first investigated. Figures 1a, 1b and 1c show the 2D plots of the temporal evolution of the photon density with continuously changing ε, g_s and g_0, the intensities of the images indicate the normalised photon densities. Figures 1d, 1e and 1f show the plots of the output pulse waveforms with certain different values of ε, g_s and g_0, corresponding to Figs 1a, 1b and 1c, respectively. Figure 1a shows that ε has almost no effect on the delay time of the pulse, but mostly affects the pulse width by changing the falling part of the pulse, more clearly, by modulating the high photon density part (peak of pulse) as shown by Fig. 1d. Figure 1b shows that g_s significantly affects the delay time in a large time region. From the plot in Fig. 1e, we can see that g_s affects not only the delay time but also the rise time of the pulse, and therefore the pulses became sharper at the rising edge with increasing g_s. Figures 1c and 1f show that the pulse shape can be also changed by varying g_0, but not so obvious compared with g_s. By comparing Fig. 1e with Fig. 1f, it can be seen that the pulse width can be changed significantly; however, it is hard to change the pulse width by changing g_0 once g_s is fixed. These

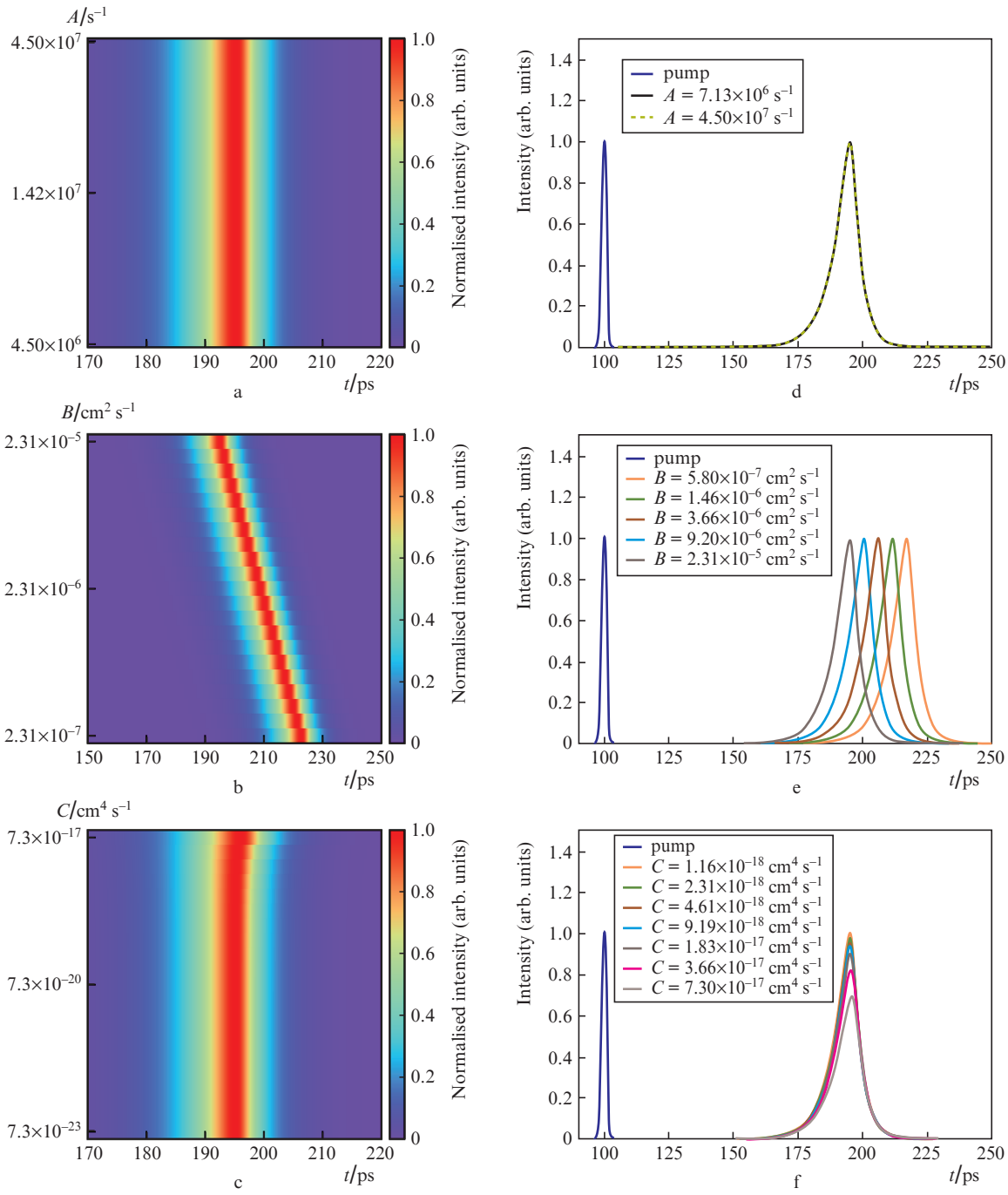

Figure 2. (Colour online) (a–c) Temporal evolution of normalised photon density and (d–f) output waveforms at different values of A, B and C.

results are in good agreement with the previous results [24], where saturation effects and average carrier lifetime were used.

Figures 2a, 2b and 2c show the photon-density normalised 2D plots of the temporal evolution of the photon density with continuously changing parameters A, B and C. Figures 2d, 2e and 2f show the plots of the output pulse waveforms with certain different values of A, B and C. It follows from Figs 2a and 2d that A hardly affects the pulse intensity and the characteristics of the pulses. Figures 2b and 2e show that the pulse delay time decreases with increasing B, while keeping the intensity and pulse width hardly changed. On the contrary, Figs 2c and 2f demonstrate that C significantly affects the pulse intensity, while hardly affects the delay time and pulse width. Therefore, we can roughly summarise the effects of A, B and C on the pulse characteristics: A nearly has no influence on the pulse delay time, pulse width and intensity; B can significantly affect the delay time; and C can significantly affect the intensity. The effects of B and C are distinctly different.

Next, in order to have a further understanding of the influence of B and C on gain-switching dynamics, we analysed the temporal evolution of carrier density, photon density and gain. Figure 3 shows the typical time evolutions of carrier density, material gain and photon density during a cycle of

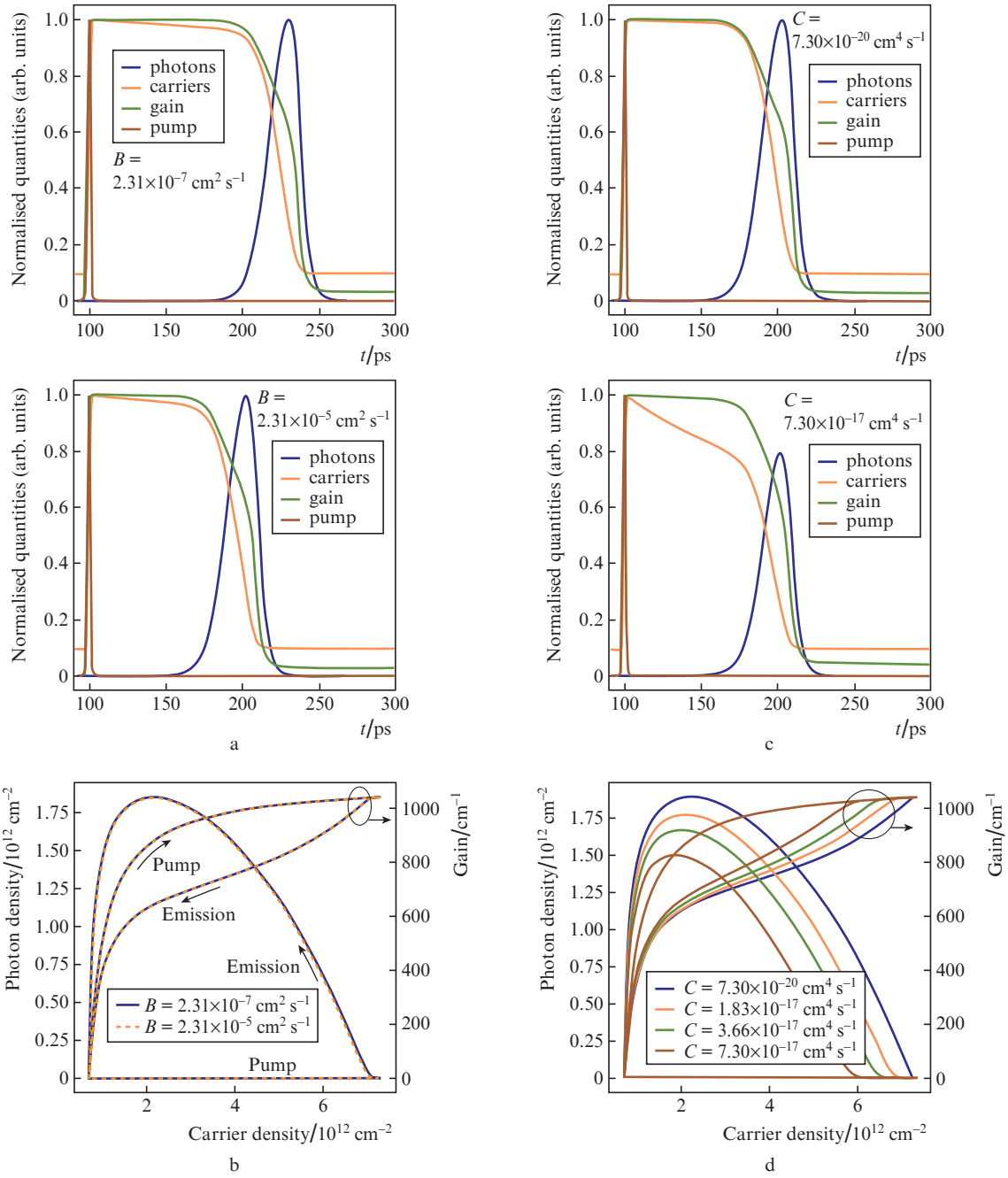

(Colour online) (a, c) Typical evolutions of carrier density (yellow), material gain (green) and photon density (blue) during a cycle of pulse generation after a 2-ps optical pulse pumping as well as (b, d) dependences of material gain and photon density on carrier density at different values of B and C. The calculation parameters are as follows: $g_0 = 3\times10^{-9}$ cm, $g_s = 1100$ cm^{-1}, $\varepsilon = 0.2\times10^{-12}$ cm^2, $A = 4.5\times10^6$ s^{-1}, as well as $B = 2.31\times10^{-5}$–10^{-7} cm^2 s^{-1} (a) and $C = 7.3\times10^{-17}$–10^{-20} cm^4 s^{-1} (c).

gain-switched pulse generation with different values of B and C. One can see from Figs 3a and 3c that, after the 2-ps pumping process, the carrier density drops smoothly before the pulse generation process. This phenomenon is caused by both radiative recombination and nonradiative recombination. In ABC model, the differential carrier lifetime τ_{diff} is given by $1/\tau_{diff} = A + 2Bn + 3Cn^2$. It shows that under higher carrier density, the effect of Auger recombination becomes more significant and carrier lifetime becomes shorter; therefore, the carrier drop with higher values of C is faster, which causes a lower peak intensity of the pulse as shown in Fig. 3c. Figure 3a shows that increasing B does not have obvious effect on the carrier-density drop but can cause a decrease in the delay time of pulse generation. This result can be understood as the initial photon density generated by spontaneous emission is higher with high values of the parameter B, and the rates of photon generation are at a relatively high level so that the stimulated emission process starts earlier. Figures 3b and 3d show the plot of photon density and gain as functions of carrier density. In Fig. 3b, the curves overlap well even at different values of the parameter B, which indicates that B hardly affects the gain-switching dynamics and the intensity of the generated pulse. In contrast, Fig. 3d shows that increasing C affects the gain-switching dynamics obviously by decreasing carrier density and accordingly decreasing optical gain, resulting in a decrease in the peak intensity of the pulse.

More detailed analysis of the temporal characteristics is shown in Figs 4 and 5. Figures 4a–4c and 5a–5c clearly demonstrate that B only affects the delay time, and does not have obvious effects on the carrier density dependence of pulse width and photon density. Figures 4d–5f and 5d–5f clearly show that C mainly affects the output power of the pulses, and does not have significant effects on the carrier density dependence of delay time and pulse width. This phenomenon is attributed to the fact that the increasing spontaneous emission enhances the initial photon density and the effect of Auger recombination on carrier lifetime is a three order term. One can also see from Figs 5f and 2f that the effect of the parameter C having a value of no less than 10^{-18} cm^4 s^{-1} is insignificant. Thus, in designing semiconductor lasers for gain-switched short-pulse generation one should keep the parameter C less than 10^{-18} cm^4 s^{-1}.

4. Conclusions

We investigated the effects of carrier recombination coefficients on gain-switched short-pulse-generation characteristics in low-dimensional semiconductor lasers under high carrier density through a rate-equation model including the ABC model. The results showed that the radiative recombination coefficient B has a strong impact on the delay time of the gain-switched-pulse, while the Auger recombination coefficient C has a strong impact on the intensity of the gain-switched-pulse. In order to obtain ultrashort and ultrafast optical pulses with high peak power, it is useful to suppress the Auger recombination and increase the radiative recombination coefficients in the design and fabrication of semiconductor laser for gain-switching operation.

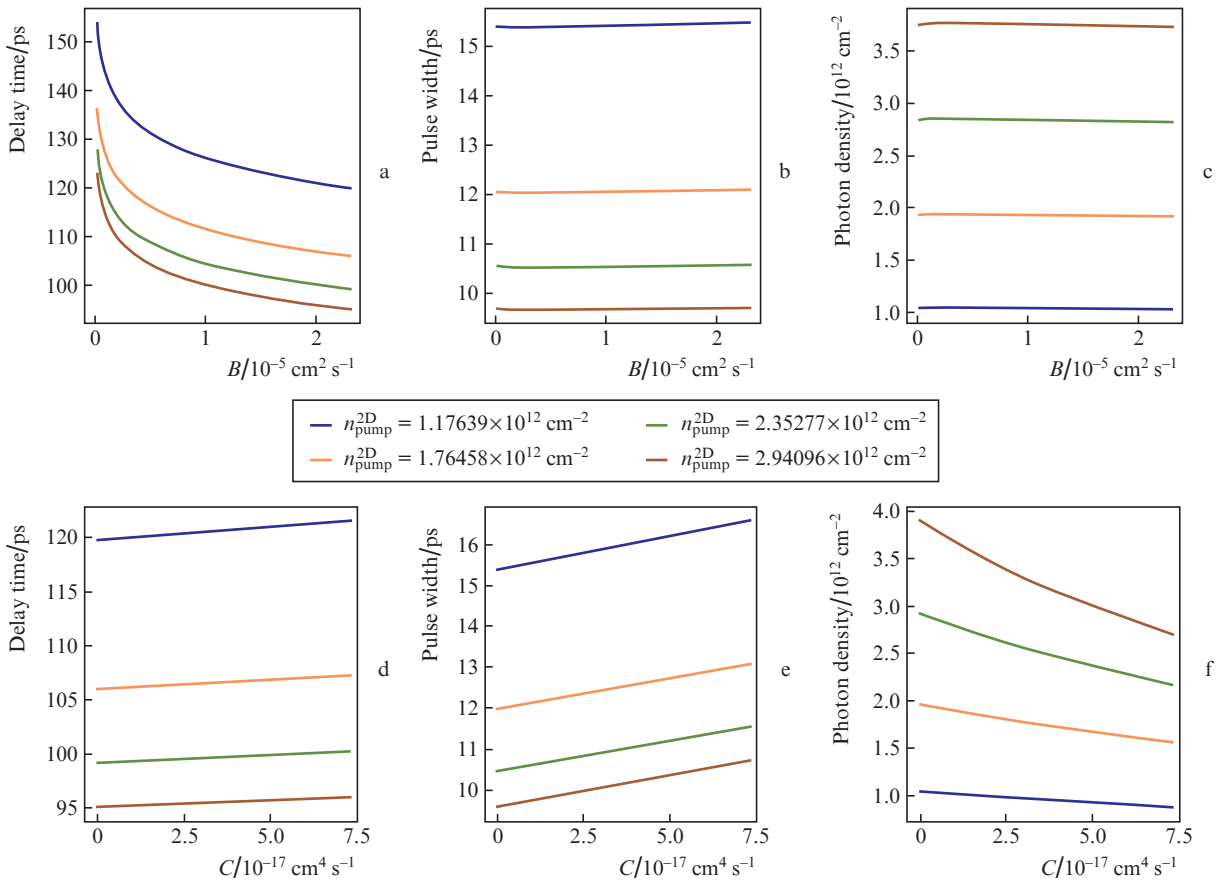

Figure 3. (Colour online) Delay time, pulse width and photon intensity as functions of the parameters B and C at different n^{2D}_{pump}.

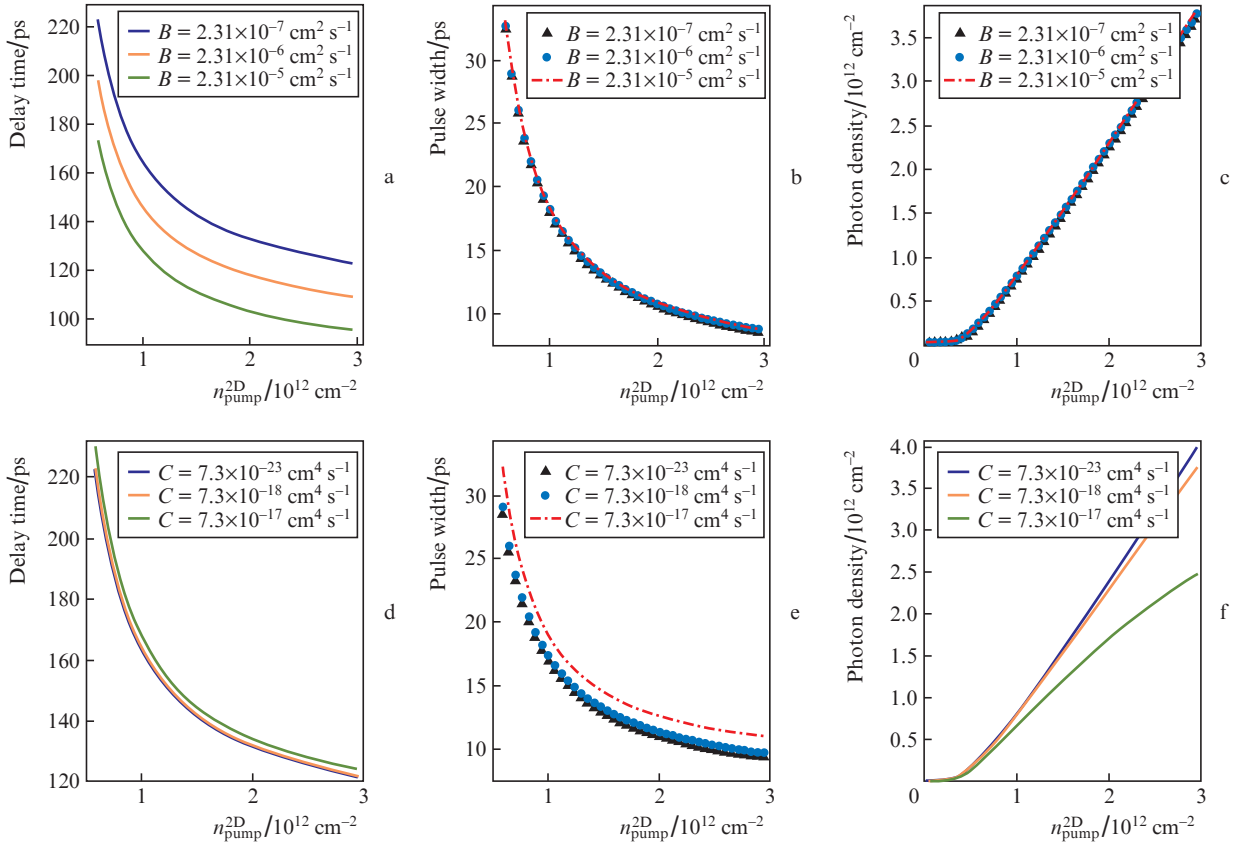

Figure 4. (Colour online) Output pulse delay time, pulse width and photon density as functions of $n_{\text{pump}}^{\text{2D}}$ at different B and C.

References

1. Haas H., Yin L., Wang Y., Chen C. *J. Lightwave Technol.*, **34**, 1533 (2016).
2. Tsonev D., Videv S., Haas H. *Opt. Express*, **23**, 1627 (2015).
3. Walker E., Dvornikov A., Coblentz K., Rentzepis P. *Appl. Opt.*, **47**, 4133 (2008).
4. Anscombe N. *Nat. Photonics*, **2**, 393 (2008).
5. Tashiro S., Takemoto Y., Yamatsu H., Miura T., Fujita G., Iwamura T., Ueda D., Uchiyama H., Yun K., Kuramoto M., Miyajima T., Ikeda M., Yokoyama H. *Appl. Phys. Express*, **3**, 102501 (2010).
6. Oka A., Shinoda K., Uomi K., Oishi A., Tsuchiya T., Komori M. *Electron. Lett.*, **30**, 2037 (1994).
7. Huang C.-C., Lin C.-F. *Proc. SPIE*, **5365**, 21 (2004).
8. Kwon O.K., Kim K.H., Sim E.D., Kim J.H., Kim H.S., Oh K.R. *IEEE Photonics Technol. Lett.*, **17**, 537 (2005).
9. Alharthi S.S., Clarke E., Henning I.D., Adams M.J. *IEEE Photonics Technol. Lett.*, **27**, 1489 (2015).
10. Liu H.-F., Fukazawa M., Kawai Y., Kamiya T. *IEEE J. Quantum Electron.*, **25**, 1417 (1989).
11. Räikkönen E., Kaivola M., Buchter S.C. *J. Eur. Opt. Soc. Rapid Publ.*, **1**, 06012 (2006).
12. Chuah C.W., Xu B., Tan T.S., Xiang N., Chong T.C. *IEEE Photonics Technol. Lett.*, **19**, 70 (2007).
13. Lau K.Y. *Appl. Phys. Lett.*, **52**, 257 (1988).
14. Chen S., Sato A., Ito T., Yoshita M., Akiyama H., Yokoyama H. *Opt. Express*, **20**, 24843 (2012).
15. Chen S., Okano M., Zhang B., Yoshita M., Akiyama H., Kanemitsu Y. *Appl. Phys. Lett.*, **101**, 191108 (2012).
16. Asahara A., Chen S., Ito T., Yoshita M., Liu W., Zhang B., Suemoto T., Akiyama H. *Sci. Rep.*, **4**, 6401 (2014).
17. Marinelli C., Khrushchev I.Y., Rorison J.M., Penty R.V., White I.H., Kaneko Y., Watanabe S., Yamada N., Takeuchi T., Amano H., Akasaki I., Hasnain G., Schneider R., Wang S.Y., Tan M.R.T. *Electron. Lett.*, **36**, 83 (2000).
18. Kono S., Oki T., Miyajima T., Ikeda M., Yokoyama H. *Appl. Phys. Lett.*, **93**, 131113 (2008).
19. Oki T., Kono S., Kuramoto M., Ikeda M., Yokoyama H. *Appl. Phys. Express*, **2**, 032101 (2009).
20. Chen S., Ito T., Asahara A., Yoshita M., Liu W., Zhang J., Zhang B., Suemoto T., Akiyama H. *Sci. Rep.*, **4**, 7888 (2014).
21. Shen Y.C., Mueller G.O., Watanabe S., Gardner N.F., Munkholm A., Krames M.R. *Appl. Phys. Lett.*, **91**, 141101 (2007).
22. David A., Grundmann M.J. *Appl. Phys. Lett.*, **96**, 103504 (2010).
23. Piprek J. *IEEE J. Quantum Electron.*, **53**, 1 (2016).
24. Chen S., Yoshita M., Ito T., Mochizuki T., Akiyama H., Yokoyama H., Kamide K., Ogawa T. *Jpn. J. Appl. Phys.*, **51**, 098001 (2012).
25. Piprek J., Römer F., Witzigmann B. *Appl. Phys. Lett.*, **106**, 101101 (2015).
26. Asryan L.V. *Quantum Electron.*, **35**, 1117 (2005) [*Kvantovaya Elektron.*, **35**, 1117 (2005)].
27. Williams K.W., Monahan N.R., Koleske D.D., Crawford M.H., Zhu X.-Y. *Appl. Phys. Lett.*, **108**, 141105 (2016).
28. Dai Q., Shan Q., Cho J., Schubert E.F., Crawford M.H., Koleske D.D., Kim M.-H., Park Y. *Appl. Phys. Lett.*, **98**, 33506 (2011).
29. Nippert F., Karpov S., Pietzonka I., Galler B., Wilm A., Kure T., Nenstiel C., Callsen G., Straßburg M., Lugauer H.-J., Hoffmann A. *Jpn. J. Appl. Phys.*, **55**, 05FJ01 (2016).